Diffraction imaging using reverse time migration with poynting vectors

Wenbin Jiang, Zhiyang Liu, Jie Zhang. University of Science and Technology of China (USTC)*

Summary

Seismic diffractions and reflections present different responses in the dip-angle common image gathers (dip-angle CIGs). The recognition and separation of two types of data might reveal high-resolution information of the subsurface properties. In this study, we present a diffraction imaging method based on reverse time migration (RTM) with poynting vectors. We first calculate the dip angle between the vertical axis and the normal direction of the reflector by using poynting vectors. The dip-angle CIGs are formed by binning the migrated energy. Then, we apply a median filter to suppress the focused reflection energy. Finally, we obtain the diffraction image by stacking the filtered dip-angle CIGs. We demonstrate the effectiveness of the proposed method using two examples.

Introduction

Reflections are widely employed for imaging the interior of the earth. Diffractions carry information from fault, fracture zones, and erosional surface (Kozlov et al., 2004). It is often helpful for making geological interpretation if we can distinguish these two types of data and produce imaging results separately (Schoepp et al., 2014; Popovici et al., 2015). However, one fundamental challenge of diffraction imaging is that the diffraction energy is usually much weaker than the reflection. Therefore, it is crucial to separate diffractions from reflections.

In recent years, many methods have been proposed to improve the performance of diffraction imaging. (Harlan et al., 1984; Landa et al., 1987; Khaidukov et al., 2004; Moser and Howard, 2008; Taner et al., 2006; Sturzu et al., 2014). Some methods try to separate diffractions from reflections by utilizing their differences of the kinematic and dynamic properties. Other methods utilize migrated dip-angle CIGs to image diffractors (Landa et al. 2008; Reshef and Landa 2009; Klokov, Baina, and Landa 2010; Klokov and Fomel 2012). However, these methods are based on ray-theory, which may fail to image complex geological areas. Ray-theory is based on high-frequency approximation. In this assumption, the wavelength is much smaller than the scale of scattered structures, which often leads to the nonexistence of diffraction. On the other hand, the wave-equation based methods are capable of imaging complex areas with improved accuracy. Silvestrov et al (2015) propose a method to separate diffraction and reflection by using surface angle CIGs from poststack RTM. Liu et al (2016) develop diffraction imaging method based on wave equation migration.

In this study, the poynting vector is applied to calculate the scattering angle between incident wave and scattered wave, and the angle between incident wave and vertical direction. Then, we form the dip-angle CIGs, and filter the reflection energy. Finally, we stack the filtered gathers to produce diffraction images. In the following sections, we will present basic theory, and demonstrate the algorithm with synthetic examples.

Theory

In the 2D case, we often obtain the scatter-angle common image gathers (scatter-angle CIGs) by calculating half open angles in migration. However, it is difficult to distinguish diffractions from reflections in scatter-angle CIGs. Both reflections and diffractions appear flat if the correct migration velocities are applied. While in the dip-angle domain, the specular reflections will focus at the dip angle of the reflector. In contrast, the diffraction energy will spread as a flat event due to multi-angle scattering (Liu et al., 2016; Dafni and Symes 2016). We can distinguish the seismic diffractions and reflections by their unique dip angle response.

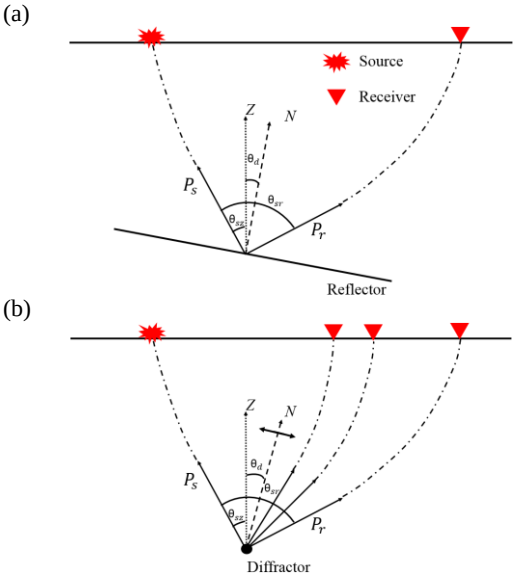

Figure 1. Sketches of the dip angle in reflection and diffraction cases. θ_{sr} is the scattering angle between incident wave and scattered wave. θ_{sz} is the angle between incident wave and vertical direction. θ_d represent the dip angle between the vertical axis and the normal direction of the reflector/diffractor. (a) reflection case. (b) diffraction case.

Diffraction imaging using reverse time migration

A reflector can be considered as a combination of continuous scatters. The scattered waves interfere with each other and generate the reflection wave. Figure 1 illustrates how the incident wave generates reflections and diffractions. The specular reflection correspond to a particular dip angle (Figure 1a). Thus, the reflection response appears to be concentrated energy in dip-angle CIGs. In contrast, the diffractions correspond to different dip angles, due to multi-angle scattering (Figure 1b). Therefore, the diffraction energy becomes a flat event in dip-angle CIGs.

In RTM, the poynting vectors are often applied to calculate wave propagation direction (Yoon and Marfurt, 2006). The definition of the poynting vector is

$$\mathbf{P} = -\nabla u \frac{\partial u}{\partial t} u \quad (1)$$

In this study, we apply the poynting vector to calculate the scattering angle θ_{sr} and incident angle θ_{sz} at every imaging point. The dip angle can be expressed as:

$$\theta_d = \frac{\theta_{sr}}{2} - \theta_{sz} \quad (2)$$

where θ_d represents the dip angle between the vertical axis and the normal direction of the reflector/diffractor. We obtain the dip-angle CIGs by binning the migration images according to the calculated dip angles. A median filter is applied to the dip angle gathers to separate the diffraction energy (Liu et al., 2016). Finally, we stack the dip-angle CIGs to obtain a migration image without reflection energy. Moreover, the poynting vector can be utilized to suppress the low wavenumber features in the dip angle domain, and improve the quality of diffraction migration image.

Synthetic Examples

We apply the proposed method to a three layer model with a point diffractor. The interface between first layer and second layer presents a -12º dip angle. The second interface is flat. Figure 2a shows the velocity model. Figure 2b and 2c depict the conventional RTM image and diffraction image separately. Both interfaces and the diffractor are clearly revealed in the RTM image. While in the diffraction image, the reflection energy is removed. It helps us better image the small-scale diffractor.

Figure 3a illustrates the dip angle gathers at the position of 500 m, 750 m and 1000 m. We observe that the reflection energy focuses at the correct reflector depth with a correct dip angle. In addition, we note that there are low wavenumber features in the top of dip angle gathers (Figure 3a). An angle filter is applied to suppress these low-wavenumber features (Figure 3b). The diffraction energy spreads as a flat event in the dip-angle CIGs. We also apply the median filter to the dip-angle CIGs to remove the focused reflection energy (Figure 3c).

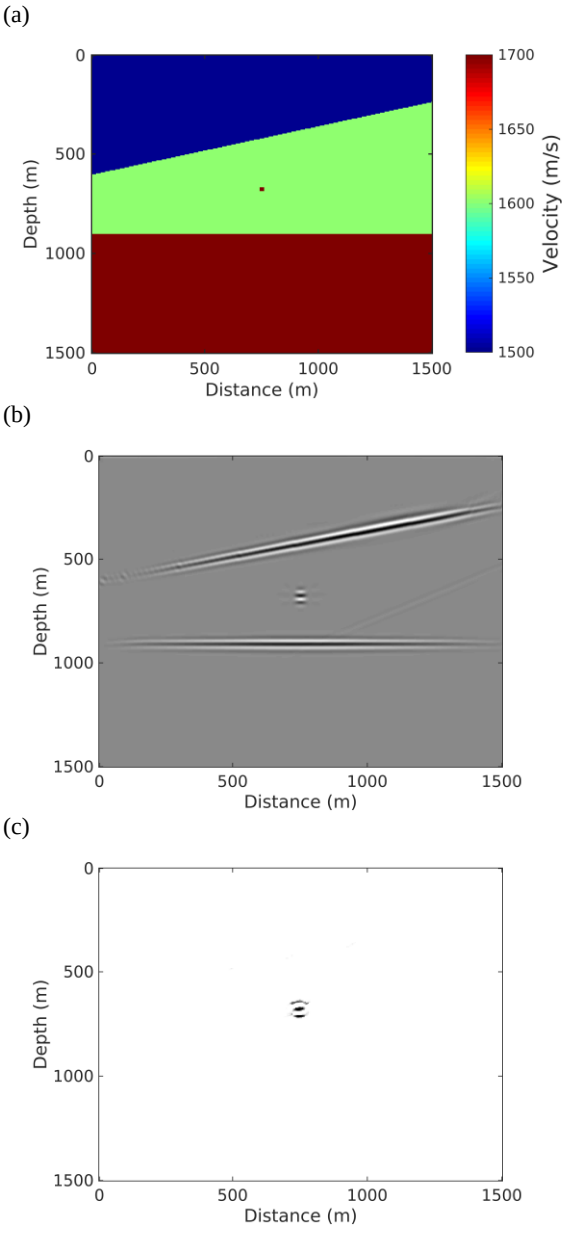

Figure 2. (a) Velocity model. (b) Conventional RTM image. (c) Diffraction image.

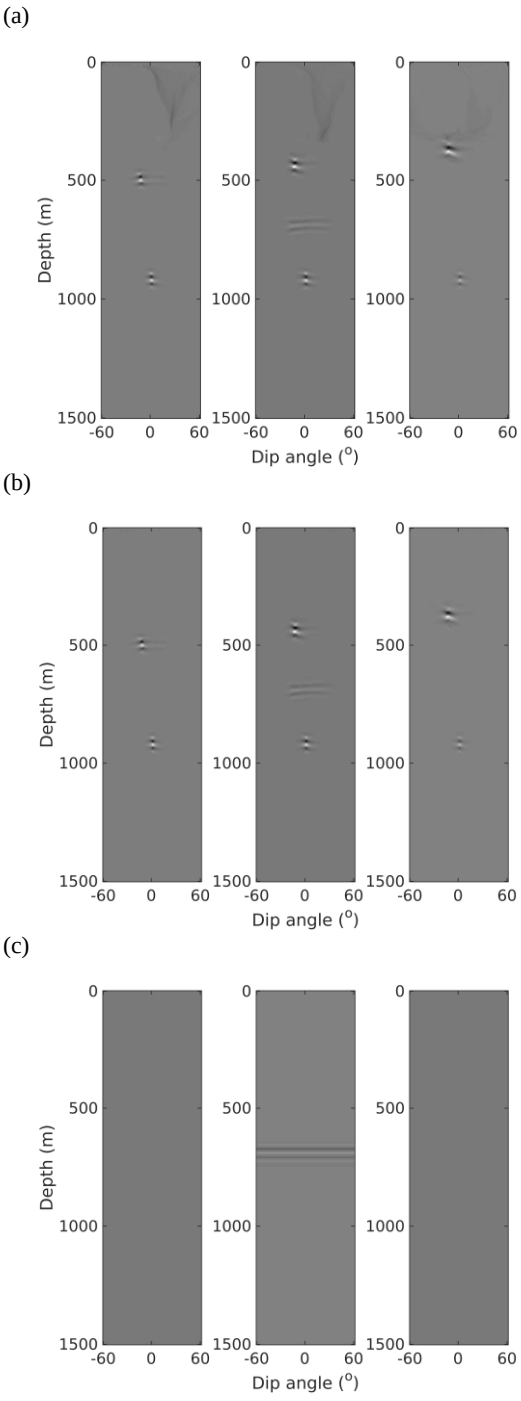

Figure 3. Dip angle gathers at the location of 500 m, 750 m and 1000 m. (a) Dip angle gathers. (b) Apply angle filter to remove low frequency noise in dip angle gathers. (c) Dip angle gathers after diffraction separation.

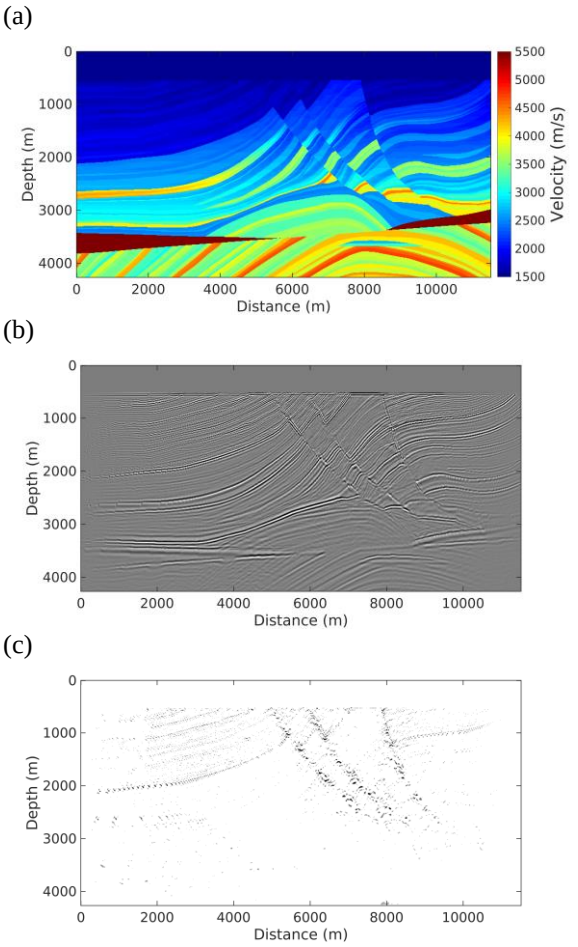

Figure 4. (a) Marmousi model. (b) Conventional RTM image. (c) Diffraction image.

To validate the performance to image complex geological areas, we apply our method to the Marmousi model. We generate 112-shot data with a Ricker wavelet of 20 Hz. There are 1152 receivers for each shot along surface with a 10 m interval. The maximum recording time is 5.0 s.

Figure 4a and 4b show the migration velocity model and conventional RTM image, respectively. Figure 4c depicts the diffraction image obtained by following the same steps as in the previous example. The diffraction events along faults and local discontinuities are clearly imaged in the figure. It indicates that our diffraction imaging method has a high resolution for revealing the small-scale diffractors.

Figure 5a shows the dip-angle CIGs at the location of 2000 m. We also apply the median filter to the dip angle gathers. The focused reflection energy is suppressed (Figure 5b).

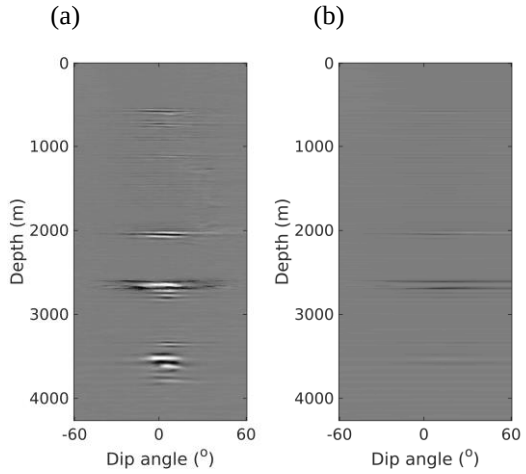

Figure 5. Dip angle gathers at the location of 2000 m. (a) Dip angle gathers. (b) Dip angle gathers after separate diffraction energy.

Conclusions

We develop a method for imaging diffraction objects in complex geological areas. The proposed method is based on a separation between the specular reflection and diffraction in dip-angle CIGs. We calculate the dip angle between the vertical axis and the normal direction of the reflector by poynting vectors, and obtain the dip-angle CIGs by binning the RTM images according to the calculated dip angles. Then, we employ a median filter to suppress the focused reflection energy on the dip angle gathers. Finally, we stack dip-angle CIGs to obtain the diffraction imaging. The results of two examples illustrate that the diffraction imaging can help to interpret discontinuous structures in complex geologic zones.